



# Adaptive mesh refinement for finite-volume discretizations with scalene triangles

Sanderson L. Gonzaga de Oliveira and Guilherme Oliveira Chagas

Departamento de Ciência da Computação, Universidade Federal de Lavras, Lavras, MG, Brazil,  
[sanderson@dcc.ufla.br](mailto:sanderson@dcc.ufla.br), [guilherme.o.chagas@gmail.com](mailto:guilherme.o.chagas@gmail.com)

## Abstract

In this work, simulations with scalene triangle meshes represented by a recently proposed graph-based adaptive mesh refinement technique are described. Previously, simulations exclusively with isosceles right triangles were presented with this graph-based scheme. This data structure represents triangular meshes in finite-volume discretizations in order to solve second-order partial differential equations. The main advantages of using this graph-based adaptive triangular mesh refinement technique are that low computational cost to adapt and traverse the mesh and low computational storage cost are achieved. This paper is a result of a work in modeling the Laplace equation with scalene triangles.

**Keywords:** Adaptive mesh refinement, mesh generation, non-conformal mesh, elliptic boundary value problem, Laplace equation

## 1 Introduction

Development of methods to control and adjust level of details of a data set is a very active research area. This occurs mainly because of the growing need of analysis and visualization of details of complex data sets, such as geometric shapes, geographic models or volumetric scalar fields [3].

De Floriani et al. [3] also explain that many applications require operations of data extraction in real time or at least on-line for structures that in general have complicated geometries. Requirements of performance and scalability impose several challenges in the design of a system of this nature. In general, a better approximation to the solution is directly proportional to the computational and storage costs of the solution. Taking scalability into account, one needs to balance these characteristics to find a generic and flexible model. Generally, the choice of the data structure depends on the application, expected performance, data size and operations to be performed. In particular, triangles are easier to be stored than more complicated polygons.

Adaptive mesh refinement techniques associated to finite volume discretizations are frequently applied to concentrate more polytopes in specific regions than in other regions of the mesh. Certainly, inserting properly more polytopes only in specific regions of the mesh must

preserve the accuracy of the solution with the benefits that low computational and storage costs are attained. This occurs mainly because the resulting linear system is smaller when applying an adaptive mesh refinement technique than when employing a mesh refined uniformly. Furthermore, adaptive mesh refinement is a very active field of research; recent examples include the works by Bryan et al. [2], Kopera and Giraldo [9], Fakhari and Lee [4], and Gonzaga de Oliveira and Kischinhevsky [7]. Gonzaga de Oliveira et al. [6] recently proposed a graph to represent the adaptive triangular mesh refinement in the finite volumes discretizations of second-order partial differential equations. The main advantages of using this graph are that low computational cost to adapt and traverse the mesh and low computational storage cost are achieved. On the other hand, the triangle shapes affect accuracy and Gonzaga de Oliveira et al. [6] presented simulations exclusively with isosceles right triangles; they did not show if other types of triangles could be used with this set of techniques for discretizations of second-order partial differential equations. In this present work, the Laplace equation is solved by this scheme: finite-volume discretizations and this graph-based adaptive mesh refinement; however, *scalene* triangles are used instead of isosceles right triangles.

Section 2 gives details about the scheme developed in this work. The experiments performed are addressed in Section 3. Final remarks are shown in Section 4.

## 2 Scheme development

Likewise carried out in Gonzaga de Oliveira et al. [6], hanging nodes are allowed and, consequently, non-conformal meshes are allowed in the finite volume discretizations used in this work. Furthermore, scalene-triangular meshes are dynamically generated and the mesh generation depends on the simulation. Moreover, quality of the scalene-triangular control volumes is controlled by the algorithms of the adaptive mesh refinement and the meshes remain smooth. Furthermore, similarly to performed by Gonzaga de Oliveira et al. [6], during the adaptive mesh refinement process, the *four triangle longest-edge* (4T-LE) partition [11] is applied. However, since a space-filling curve was not applied in this mesh, the graph vertices that represent the control volumes are ordered by the Cuthill-McKee reverse algorithm [5].

Including, linear system solvers based on the minimization of functionals can be easily applied in conjunction with the set of techniques. Specifically, the Jacobi preconditioned conjugate gradient method [8, 10] was employed.

Additionally, the same cell-centered triangular finite-volume approximation applied in Gonzaga de Oliveira et al. [6] was used. It is an extended finite-volume approach proposed by Schneider and Maliska [12] for the solution of PDEs with low computational cost.

## 3 Experiments

Let's consider the Dirichlet problem given by  $\nabla^2 \phi = 0$  in  $\Omega \in \mathbb{R}^2$ ,  $\phi = f$  on  $\partial\Omega$ , where  $\phi$  is the dependent variable of the partial differential equation,  $\Omega$  is a limited domain in  $\mathbb{R}^2$ , and  $f$  is a defined smooth function on the boundary  $\partial\Omega$ . This problem is well-posed in the Hadamard sense [13]. The prescribed boundary conditions were set as  $f(0, y) = f(x, 0) = f(x, 1) = 10$  and  $f(1, y) = 0$ . This problem was solved by finite-volume discretizations and examples of the generated meshes are shown below. A color map is shown in Figure 1. This color scheme was used in the meshes generated.

The initial grid is composed of scalene triangles, as exemplified in Figure 2. Examples of refined meshes composed of 32 (1 refinement level allowed), 119 (2 refinement levels allowed),



Figure 1: Color map used to represent the approximation to the Laplace equation solutions in the meshes.

449 (3 refinement levels allowed), 1265 (4 refinement levels allowed), 3551 (5 refinement levels allowed), 8194 (6 refinement levels allowed) control volumes are shown in Figures 3 - 8, respectively.

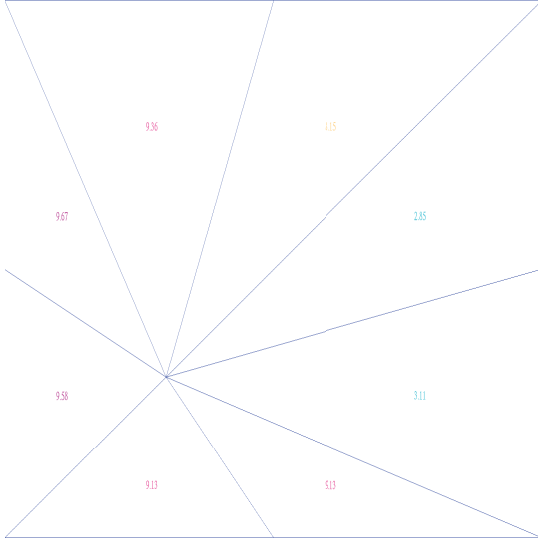


Figure 2: Example of an initial mesh composed of scalene triangles and the solution (approximated in the second decimal place) of the Laplace equation by finite volume discretizations.

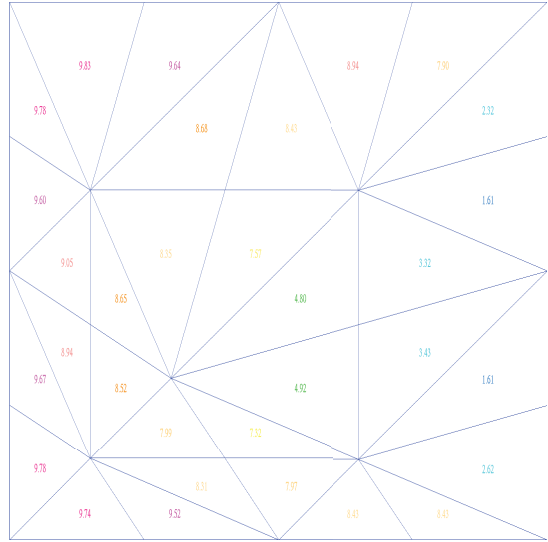


Figure 3: Mesh composed of 32 scalene triangles and the solution (approximated in the second decimal place) of the Laplace equation by finite volume discretizations.

A refined mesh composed of 13043 scalene-triangle control volumes is shown in Figure 9. In this simulation, the refinement criterion was set as 0.69 (instead of 0.31 as in the previous simulations) and 16 refinement levels were allowed; hence, more triangles were concentrated in the right corners of the mesh.

This scheme using scalene triangles resulted in higher computational cost than the original isosceles right triangles presented by Gonzaga de Oliveira et al. [6]. However, a feasible computational time was reached; e.g. computational costs to solve some linear system in an Intel® Core™ i7-2670QM CPU @ 2.20GHz with 8GB of memory are shown in Table 1.

Table 1: Computational costs of some simulations:  $N$  is the number of scalene-triangle control volumes and time is given in seconds.

$N$	11066	12119	13043
Time (s)	71.8	87.4	111.9

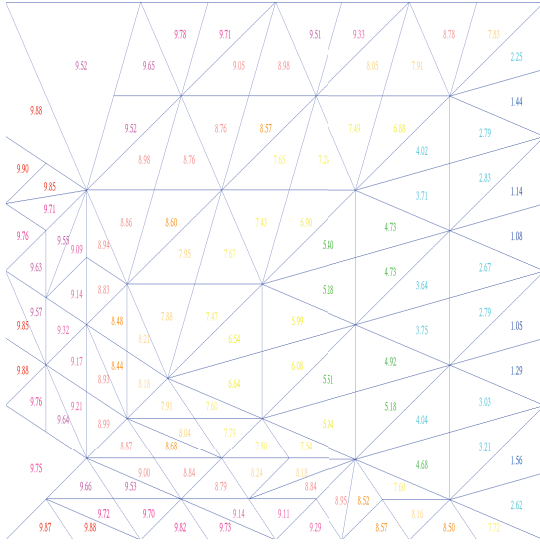


Figure 4: Mesh composed of 119 scalene triangles and the solution (approximated in the second decimal place) of the Laplace equation by finite volume discretizations.

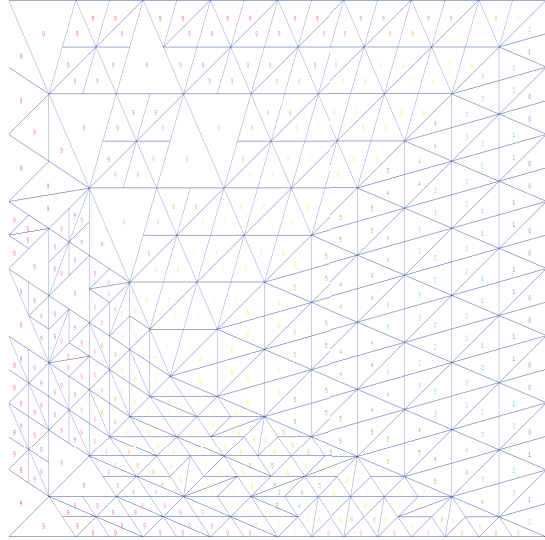


Figure 5: Mesh composed of 449 scalene triangles and the solution of the Laplace equation by finite volume discretizations.

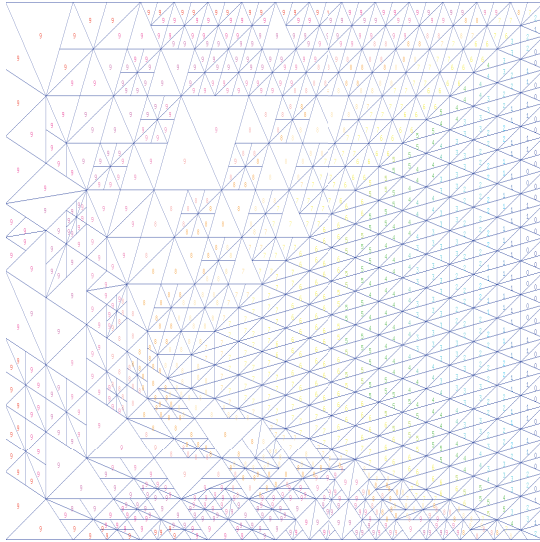


Figure 6: Mesh composed of 1265 scalene triangles and the solution of the Laplace equation by finite volume discretizations.

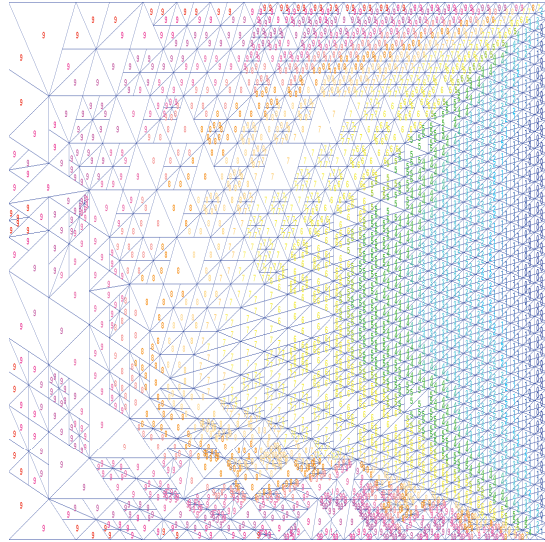


Figure 7: Mesh composed of 3551 scalene triangles and the solution of the Laplace equation by finite volume discretizations.

Similarly, the resulting refined mesh of other simulation is shown in Figure 10. In this simulation, the refinement bound was decreased to  $10^{-14}$ , instead of  $10^{-9}$  as used in the previous simulations. In Table 2, the quantity of triangles per quality in several simulations are shown.

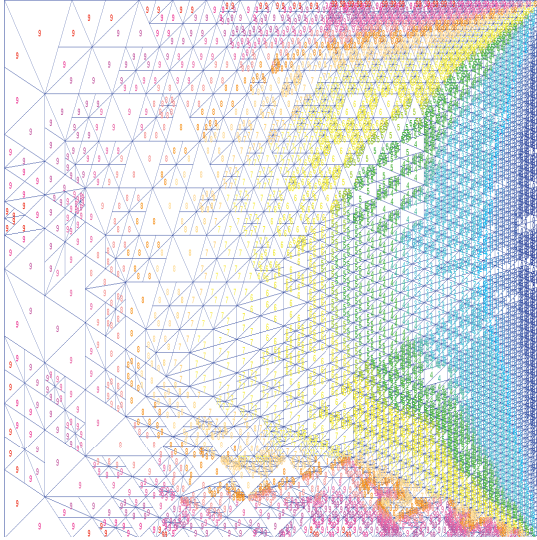


Figure 8: Mesh composed of 8194 scalene triangles and the solution of the Laplace equation by finite volume discretizations.

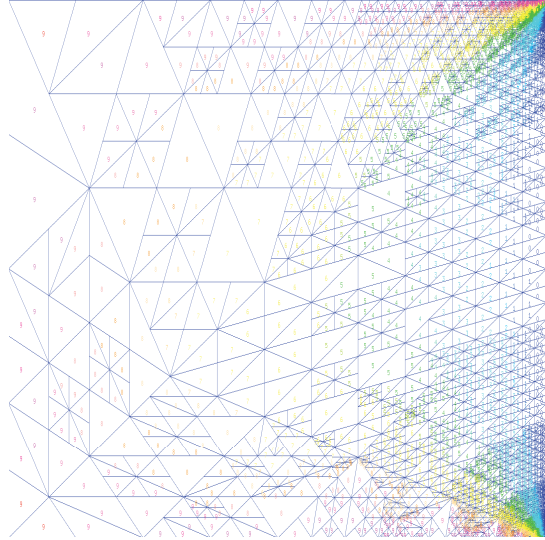


Figure 9: Mesh composed of 13043 scalene triangles and the solution of the Laplace equation by finite volume discretizations.

The quality of the triangles was measured by the scheme of Bank e Smith [1], which can be defined as  $q = \frac{4\sqrt{3}A}{l_1^2 + l_2^2 + l_3^2}$ , where  $A$  is the area and  $l_1, l_2$  e  $l_3$  are the sides of the triangle. These simulations were executed in an Intel® Core™i3 CPU 550 @ 3.20GHz with 16GB of memory.

More than 53% of the control volumes are comprised of high-quality triangles, almost 44% of the control volumes are comprised of medium-quality triangles, and approximated 3% are low-quality triangles, in these simulations. The low-quality triangles could be refined in order to improve the quality of the mesh. However, only triangles related to the refinement criterion were refined in these simulations so that more control volumes are concentrated in the two right corners of the computational domain due to the boundary conditions applied.

## 4 Conclusions

Simulations with a recent graph-based adaptive mesh refinement scheme for discretizations of second-order partial differential equations were described. Gonzaga de Oliveira et al. [6] presented simulations only with isosceles right triangles. Meshes presented by the authors did not show if other types of triangles as control volumes could be applied with this set of techniques for finite-volume discretizations of second-order partial differential equations. In this present work, solutions of the Laplace equation by this graph-based finite-volume discretization scheme applying scalene-triangle control volumes were shown.

In a future work, other second-order partial differential equations shall be applied, e.g. heat conduction and wave equations. In addition, higher-order approximation is intended to be used. Specifically, the weighted essentially non-oscillatory scheme shall be applied.



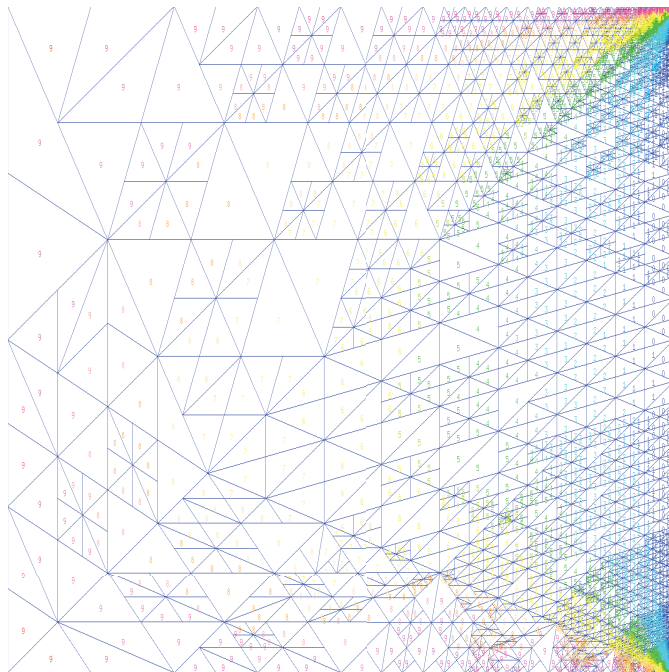


Figure 10: Mesh composed of 23684 scalene triangles and the solution of the Laplace equation by finite volume discretizations.

$q$	(0.4,0.5]	(0.5,0.6]	(0.6,0.7]	(0.7,0.8]	(0.8,0.9]	(0.9,1.0]	Total	$l$	$B$	Time (s)
$N$	150	288	5697	502	6556	1017	14210	17	$10^{-10}$	114.9
%	1.1	2.0	40.1	3.5	46.1	7.2	100	-	-	-
$N$	160	306	6135	539	7057	1087	15284	18	$10^{-11}$	135.8
%	1.1	2.0	40.1	3.5	46.2	7.1	100	-	-	-
$N$	190	349	6555	637	7546	1270	16547	19	$10^{-12}$	158.8
%	1.1	2.1	39.6	3.9	45.6	7.7	100	-	-	-
$N$	180	342	6979	613	8034	1227	17375	20	$10^{-13}$	175.4
%	1.0	2.0	40.2	3.5	46.2	7.1	100	-	-	-
$N$	190	360	7403	650	8528	1297	18428	21	$10^{-14}$	199.7
%	1.0	2.0	40.2	3.5	46.3	7.0	100	-	-	-
$N$	220	403	7837	748	9024	1480	19712	22	$10^{-15}$	228.2
%	1.1	2.0	39.8	3.8	45.8	7.5	100	-	-	-
$N$	210	396	8247	724	9505	1437	20519	23	$10^{-16}$	250.7
%	1.1	1.9	40.2	3.5	46.3	7.0	100	-	-	-
$N$	220	414	8685	761	10006	1507	21593	24	$10^{-17}$	272.1
%	1.0	1.9	40.2	3.5	46.4	7.0	100	-	-	-
$N$	250	457	9105	859	10495	1690	22856	25	$10^{-18}$	331.2
%	1.1	2.0	39.8	3.8	45.9	7.4	100	-	-	-
$N$	240	450	9529	835	10983	1647	23684	26	$10^{-19}$	327.4
%	1.0	1.9	40.2	3.5	46.4	7.0	100	-	-	-

Table 2: Number of triangles ( $N$ ), their quality  $q$ , refinement bound  $B$ , refinement levels ( $l$ ) allowed, and the computational cost, in seconds, demanded to solve the linear systems associated to the meshes in several simulations.

## Acknowledgments

This work was performed with the support of the CNPq - Conselho Nacional de Desenvolvimento Científico e Tecnológico (National Council for Scientific and Technological Development) and FAPEMIG - Fundação de Amparo à Pesquisa do Estado de Minas Gerais (Minas Gerais Research Support Foundation).

## References

- [1] R. E. Bank and R. K. Smith. Mesh smoothing using a posteriori error estimates. *SIAM Journal on Numerical Analysis*, 34(3):979–997, 1997.
- [2] G. L. Bryan, M. L. Norman, B. W. O’Shea, T. Abel, J. H. Wise, M. J. Turk, D. R. Reynolds, D. C. Collins, P. Wang, S. W. Skillman, B. Smith, R. P. Harkness, J. Bordner, J. Kim, M. Kuhlen, H. Xu, N. Goldbaum, C. Hummels, A. G. Kritsuk, E. Tasker, S. Skory, C. M. Simpson, O. Hahn, J. S. Oishi, G. C. So, F. Zhao, R. Cen, Y. Li, and The Enzo Collaboration. Enzo: An adaptive mesh refinement code for astrophysics. *The Astrophysical Journal Supplement Series*, 211(2):19, 2014.
- [3] L. De Floriani, L. Kobbelt, and E. Puppo. A survey on data structures for level-of-detail models. In N. Dodgson, M. Floater, and M. Sabin, editors, *Advances in Multiresolution for Geometric Modelling and Visualization*, Series in Mathematics and Visualization, pages 49–74, New York, 2004. Springer Verlag.
- [4] A. Fakhari and T. Lee. Finite-difference lattice boltzmann method with a block-structured adaptive-mesh-refinement technique. *Physical Review E*, 89(3):033310, March 2014.
- [5] J. A. George. *Computer implementation of the finite element method*. PhD thesis, Computer Science Department, Stanford University, CA, USA, 1971.
- [6] S. L. Gonzaga de Oliveira, M. Kischinhevsky, and J. M. R. S. Tavares. Novel graph-based adaptive triangular mesh refinement for finite-volume discretizations. *CMES: Computer Modeling in Engineering & Sciences*, 95(2):119–141, 2013.
- [7] S. L. G. Gonzaga de Oliveira and M. Kischinhevsky. Autonomous leaves graph applied to the simulation of the boundary layer around a non-symmetric naca airfoil. In B. Murgante, O. Gervasi, S. Misra, N. Nedjah, A. M. A. C. Rocha, D. Taniar, and B. O. Apduhan, editors, *12th International Conference on Computational Science and Its Applications, ICCSA*, volume 7333 of *LNCS*, pages 610–619, Salvador; Brazil, June 2012. Springer.
- [8] M. R. Hestenes and E. Stiefel. Methods of conjugate gradients for solving linear systems. *Journal of Research of the National Bureau of Standards*, 49(36):409–436, 1952.
- [9] M. A. Kopera and F. X. Giraldo. Analysis of adaptive mesh refinement for imex discontinuous galerkin solutions of the compressible euler equations with application to atmospheric simulations. *Journal of Computational Physics*, 275:92–117, October 2014.
- [10] C. Lanczos. Solutions of systems of linear equations by minimized iterations. *Journal of Research of the National Bureau of Standards*, 49(3):33–53, 1952.
- [11] M. C. Rivara. Algorithms for refining triangular grids suitable for adaptive and multigrid techniques. *International Journal for Numerical Methods in Engineering*, 20:745–756, 1984.
- [12] F. A. Schneider and C. R. Maliska. Numerical solution of bidimensional convective-diffusive problems by the Finite Volume Method using unstructured meshes (in Portuguese). In *IX Congresso Brasileiro de Engenharias e Ciências Térmicas*, volume 0346, 2002.
- [13] E. Zauderer. *Partial Differential Equations of Applied Mathematics*. Wiley-Interscience, 2nd edition, 1989.